Coupled two-layer plasmon modes induced in a single quantum well by in-plane magnetic fields

Shun-Jen Cheng and Rolf R. Gerhardts
Max-Planck-Institut für Festkörperforschung, Heisenbergstraße 1, D-70569 Stuttgart, Germany
(Received 31 August 2001; revised manuscript received 25 October 2001; published 4 February 2002)

We present a complete investigation of the collective excitations in quantum wells subject to in-plane magnetic fields **B**, based on the random phase approximation and self-consistently calculated ground states in the Hartree approximation. We find that, for a symmetric quantum well of width w, high in-plane **B** fields ($l_B \ll w$) can, besides the usual optical intrasubband plasmons (OP's), give rise to an additional branch of undamped acoustic plasmons (AP's), which does not exist in a single well without **B**. In low **B** fields ($l_B \gg w$), the magnetic-field broken symmetry of electron wave functions causes an anticrossing feature of the plasmon dispersions even in the symmetric well. In intermediate **B** fields ($l_B \lesssim w$), an unusual anisotropy effect occurs: the number of the plasmon branches depends on the angle between the magnetic field and the in-plane plasmon wave vector **q**. For $\mathbf{B} \| \mathbf{q}$, there exist two branches of plasmons (OP's and AP's), whereas only one (OP) exists for $\mathbf{B} \perp \mathbf{q}$.

DOI: 10.1103/PhysRevB.65.085307 PACS number(s): 73.20.Mf, 73.21.Fg, 78.67.De

I. INTRODUCTION

Two-dimensional electron systems (2DES's) in the presence of a magnetic field have attracted great interest for decades. Whereas 2DES's under a perpendicular magnetic field have been studied extensively, recently increasing attention has been paid to the 2DES subject to parallel magnetic fields.[1–8] However, collective excitations, as a fundamental property of 2DES's, in the presence of parallel magnetic fields have been investigated only by a limited number of experimental and theoretical works.[8–12] A theoretical difficulty with this topic is the need for an exact treatment of the k_x dependence of the wave functions that results from the magnetic fields in the y direction. Most existing theoretical methods to calculate the collective excitations of the electron systems are, however, applicable only for such a simplified model, in which the energy bands are parabolic and the wave functions $\Psi_{l,\mathbf{k}}(\mathbf{r},z)$ factorize into an in-plane part $\exp(i\mathbf{k}\cdot\mathbf{r})$ and a subband function $\psi_l(z)$, which is independent of the in-plane wave vector $\mathbf{k}=(k_x,k_y)$ [z denotes the direction perpendicular to the quantum well and $\mathbf{r}=(x,y)$ the in-plane position].[13–15]

A characteristic feature of the in-plane magnetic field $\mathbf{B}=B\hat{\mathbf{e}}_y$ in the y direction is, however, to introduce a strongly nonparabolic k_x dependence of the subband energies $E_l(\mathbf{k})=E_l(k_x)+\hbar^2k_y^2/2m^*$ and a nontrivial k_x dependence of the corresponding subband wave functions $\psi_{l,k_x}(z)$.[16] The correct treatment of these k_x dependences will allow us to describe a magnetic-field-induced transition from a one-component 2DES in a wide symmetric well at low **B** towards a two-component system at high **B**, which consists of two weakly coupled 2D electron layers located near the interfaces of the well. The magnetically induced one- to two-component transition has been observed in magnetotransport measurements of the fractional quantum Hall regime.[17] The aim of our work is to investigate the effect of this transition on the collective excitations of the electron system.

Part of the physics involved in this problem has recently been discussed by Aizin and Gumbs,[12] who considered coupled 2DES in two parallel narrow quantum wells with weak electron tunneling, subjected to an in-plane magnetic field. A tunneling coupling between the 2DES was modeled phenomenologically and evaluated perturbatively under the assumption that only a single subband wave function of each well needs to be considered. In a dynamical response calculation based on the random phase approximation (RPA), the extent and overlap of these subband wave functions were neglected in order to obtain an effective 2×2 dielectric matrix from which collective excitations were calculated. In certain limits results of Ref. 12 anticipate our findings in the two-component high-**B** limit. However, many aspects of our present work considering a single wide quantum well in an in-plane **B** field of arbitrary strength are not covered by the approach of Ref. 12 relying on the criterion of weak tunneling and small energy splitting Δ between the two lowest subbands at $\mathbf{k}=\mathbf{0}$ (Γ point).

In contrast to the phenomenological approach of Ref. 12, we start with a fully self-consistent calculation of the energy dispersion and wave functions of the 2DES in a wide symmetric quantum well, under the consideration of the bending of the conduction band by the Hartree potential caused by the electron charges in the well. Thus, we calculate, e.g., the energy splitting Δ, which was taken in Ref. 12 as an independent model parameter, and find that it depends strongly on the magnetic field and significantly increases with increasing B. Furthermore, we base our dynamical response calculation on the theoretical approach of Refs. 18 and 19, which is developed within the self-consistent-field version of the RPA (Ref. 20) to exactly treat the **k** dependence of wave functions and the nonparabolic band structure of quantum wells. Thereby, we can calculate the collective excitations of a symmetric, single quantum well subjected to parallel magnetic fields without the crude simplifying approximations of Ref. 12.

From our calculated results, several interesting **B**-induced phenomena and their dependences on the strength of **B** are revealed: (1) In a low magnetic field (the magnetic length is much larger than the well width, i.e., $l_B \gg w$), an anticrossing feature of the branches of the inter- and intrasubband plasmons is obtained due to the magnetic-field-induced plasmon

couplings, while the coupling does not exist in the symmetric quantum wells without **B**. (2) If the in-plane magnetic field is sufficiently strong ($l_B \ll w$), an additional, undamped acoustic intrasubband plasmon branch, besides the usual intrasubband (optical) plasmon branch, is induced in the long-wavelength limit. The existence of the magnetically induced acoustic plasmons is consistent with the one- to two-component transitions due to applying a tilted magnetic field, observed in the magnetotransport of the fractional quantum Hall regime.[17] (3) In an intermediate magnetic field ($l_B \lesssim w$), the plasmon dispersion is so anisotropic that the direction of the in-plane magnetic field with respect to **q** can affect not only the plasmon frequencies but also the number of the undamped plasmon branches. As $\mathbf{B}\|\mathbf{q}$, there exist two branches of the intrasubband plasmons, i.e., acoustic plasmons (AP's) and optical plasmons (OP's). In contrast, as $\mathbf{B}\perp\mathbf{q}$, the acoustic mode disappears and only one branch of the optical mode exists.

This paper is organized as follows. In the next section, we present the self-consistent Hartree theory for the quantum well in the presence of the in-plane magnetic field and the theoretical approach to determine the collective excitations in the framework of the RPA. In Sec. III, the calculated collective excitations for the low, moderate, and high magnetic field, the charge density of the plasmons, and the absorption spectra will be presented and discussed in detail. The paper is concluded in Sec. IV.

II. THEORY

A. Electronic structure

In the framework of the effective mass approximation, the Hamiltonian for an electron in a quantum well under a magnetic field $\mathbf{B}=\nabla\times\mathbf{A}$ is written as

$$H=\frac{1}{2m^*}\left(\mathbf{p}+\frac{e}{c}\mathbf{A}\right)^2+V_{QW}(z)+V_H(z), \tag{1}$$

where **A** is the vector potential, $V_{QW}(z)$ is the band-edge profile of the quantum well, and $V_H(z)$ is the Hartree potential. For the in-plane magnetic field in the y direction, $\mathbf{B}=(0,B,0)$, we take the vector potential $\mathbf{A}=(Bz,0,0)$ according to the Landau gauge. With the vector potential and the form of electron wave function $\Psi_{l,\mathbf{k}}(\mathbf{r},z)=(1/\sqrt{S})\exp(i\mathbf{k}\cdot\mathbf{r})\psi_{l,\mathbf{k}}(z)$ (S is the area of the 2D plane), the Schrödinger equation reads

$$\left[\frac{\hbar^2}{2m^*}(k_y^2-\partial^2/\partial z^2)+V_B(k_x;z)+V_{QW}(z)+V_H(z)\right]\psi_{l,\mathbf{k}}(z) =E_{l,\mathbf{k}}\psi_{l,\mathbf{k}}(z), \tag{2}$$

where $E_{l,\mathbf{k}}$ and $\psi_{l,\mathbf{k}}(z)$ are the energy and the subband wave function of the state with the subband index l and the in-plane wave vector **k**, respectively. The **B** field introduces a parabolic confinement potential

$$V_B(k_x;z)=\frac{1}{2}m^*\omega_c^2(z-z_0)^2, \tag{3}$$

with the k_x-*dependent* bottom position $z_0=-k_x l_B^2$, where $\omega_c\equiv eB/m^*c$ and $l_B\equiv(\hbar c/eB)^{1/2}$ are the cyclotron frequency and the magnetic length, respectively. Because V_B is independent of k_y, the energy and wave function of an electron can be written as $E_{l,\mathbf{k}}=\hbar^2k_y^2/2m^*+E_{l,k_x}$ and $\psi_{l,\mathbf{k}}(z)=\psi_{l,k_x}(z)$. This means that the in-plane **B** field in the y direction affects the band dispersion along $\mathbf{k}_x\perp\mathbf{B}$ but does not change the band dispersion along $\mathbf{k}_y\|\mathbf{B}$ [here, we define $\mathbf{k}_x\equiv(k_x,0,0)$ and $\mathbf{k}_y\equiv(0,k_y,0)$], and causes the dependence of the wave function on k_x.

The piecewise continuous conduction-band-edge profile V_{QW} of the quantum well is described by

$$V_{QW}(z)=\begin{cases}0, & \text{for } |z|<w/2,\\ \Delta E_c, & \text{for } |z|>w/2,\end{cases} \tag{4}$$

where ΔE_c is the conduction-band offset of the quantum well. The Hartree potential V_H is obtained by solving Poisson's equation

$$\frac{d^2V_H(z)}{dz^2}=-\frac{4\pi e^2}{\kappa}[\rho_e(z)-N_D^+(z)], \tag{5}$$

where $\rho_e(z)$ is the electron density, $N_D^+(z)$ is the density of the ionized donor impurities, and κ is the dielectric constant of GaAs. The Hartree potential causes the band bending of the well profile and thus two trianglelike confinement regions are formed at the side walls of the well. For symmetrically modulation-doped quantum wells, we assume no acceptor impurity and two doped layers with equal amount of donor impurities, which compensate the charge of all free electrons and are located symmetrically on the both sides of well. Throughout this section, a single symmetric GaAs/$Al_{0.35}Ga_{0.65}$As quantum well (conduction-band offset $\Delta E_c=0.25$ eV and electron effective mass $m^*=0.067m_0$ are taken) of width $w=75$ nm and electron density $N_e=10^{11}$ cm^{-2} is considered. According to the algorithm described in Ref. 19, we perform the self-consistent calculation to solve Eqs. (2) and (5), and obtain the electronic structure of the symmetric quantum well subject to in-plane magnetic fields. This is then taken as the ground state for the evaluation of the collective excitations within the frame of the linear-response theory of the RPA.

The calculated band structures of the quantum well under various in-plane **B** are shown in Figs. 1 and 2. In the presence of **B**, the subbands with $\mathbf{k}\|\mathbf{k}_x$ become nonparabolic and nonparallel. As B increases, the energy difference between subbands is raised. Above $B\sim1$ T, the minimum points of the lowest ($c1$) subband with **k** along the $\mathbf{k}_x$ direction are shifted to finite k_x points and a saddle point is formed at the k origin. As $B>3$ T, the nonparabolicity is so strong that only states with finite k_x are occupied and the corresponding Fermi contour is split into two (see the insets of Figs. 5 and 7).[3] Such extraordinary band structures are directly related to the k_x dependence of ψ_{l,k_x}. In finite **B**, the electrons with finite $z_0(\propto k_x)$ localized in the trianglelike confinement formed by V_H and the well edges have lower energies than those with $z_0, k_x\approx0$ located in the central part of the well,

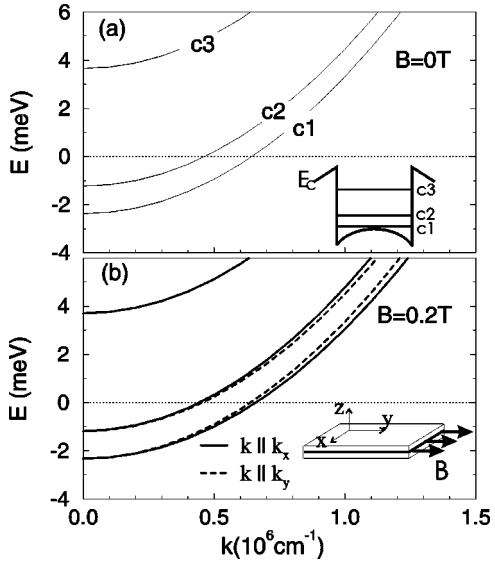

FIG. 1. Subband energies relative to the Fermi level (dotted line) for the *n*-type symmetric GaAs/$Al_{0.35}Ga_{0.65}As$ quantum well of width $w=75$ nm and electron density $N_e=10^{11}$ cm^{-2} (a) without a magnetic field and (b) with an in-plane magnetic field $B=0.2$ T in the *y* direction. Thick solid and dashed lines denote the dispersions in the $\mathbf{k}_x$ and $\mathbf{k}_y$ directions, respectively.

where the potential is raised by V_H. Thus, along $\mathbf{k}\|\mathbf{k}_x$, a $c1$ dispersion with local minimum at finite k_x results. This feature of the band structure has been investigated previously and more detailed discussions can be found, e.g., in Refs. 3,16,21, and 22. We find that the band structure in our case (see Figs. 1 and 2) with large Δ $(=E_{c2,\mathbf{0}}-E_{c1,\mathbf{0}})$ does not meet the situation considered in Ref. 12, in which very weak tunneling between wells is assumed and the energy gap Δ is much smaller than the energy difference between the middle point of the gap $[(E_{c2,\mathbf{0}}+E_{c1,\mathbf{0}})/2]$ and the local minimum energy of E_{c1} at some nonzero $\mathbf{k}$.

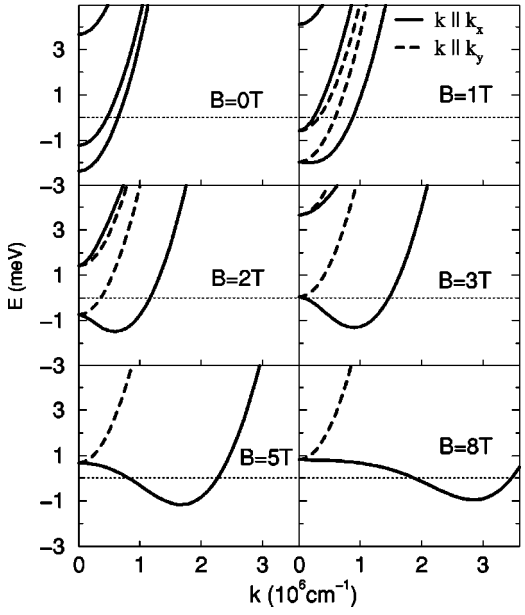

FIG. 2. The dispersion of the subband energies relative to the Fermi level (dotted line) for different values of the magnetic field *B* in the *y* direction. Well parameters and notation as in Fig. 1.

B. Collective excitations

To evaluate the dynamical screening of the quantum well under in-plane magnetic fields we take the method in Ref. 18, which can deal with the $\mathbf{k}$ dependence of the wave functions exactly, within the RPA. Following Ref. 18, a dielectric function $\epsilon_{\mathbf{q},\omega}(z;z')$, defined by

$$V^{ex}_{\mathbf{q},\omega}(z)=\int dz'\,\epsilon_{\mathbf{q},\omega}(z;z')V^{sc}_{\mathbf{q},\omega}(z'), \tag{6}$$

is used to evaluate the screening of the 2D system, where $V^{ex}_{\mathbf{q},\omega}$ $(V^{sc}_{\mathbf{q},\omega})$ is the potential induced by the external (self-consistent or screened) longitudinal electric field with in-plane wave vector $\mathbf{q}$ and frequency ω. In the spirit of the RPA, the charge density $n^{ind}_{\mathbf{q},\omega}$ induced by the external field is treated as the linear response of the noninteracting system to $V^{sc}_{\mathbf{q},\omega}$, i.e., $n^{ind}_{\mathbf{q},\omega}(z)=\int dz'\Pi_{\mathbf{q},\omega}(z;z')V^{sc}_{\mathbf{q},\omega}(z')$, where $\Pi_{\mathbf{q},\omega}$ is the noninteracting polarization function. Because $V^{sc}_{\mathbf{q},\omega}(z)=V^{ex}_{\mathbf{q},\omega}(z)+V^{ind}_{\mathbf{q},\omega}(z)$, where V^{ind} is the Coulomb potential induced by n^{ind} and given by

$$V^{ind}_{\mathbf{q},\omega}(z)=\int dz'\,W_q(z-z')n^{ind}_{\mathbf{q},\omega}(z'), \tag{7}$$

where $W_q(z-z')=v_q\exp(-q|z-z'|)$ with $v_q=2\pi e^2/(\kappa q)$ is the Coulomb interaction, we can express the dielectric function as

$$\epsilon_{\mathbf{q},\omega}(z;z')=\delta(z-z')-\int d\bar{z}W_q(z-\bar{z})\Pi_{\mathbf{q},\omega}(\bar{z};z'). \tag{8}$$

According to the standard time-dependent linear response theory,[20] the noninteracting polarization function $\Pi_{\mathbf{q},\omega}(z;z')$ is obtained as

$$\Pi_{\mathbf{q},\omega}(z;z')=\sum_{l,l'}\sum_{\mathbf{k}}\psi^*_{l,\mathbf{k}}(z)\psi_{l',\mathbf{k}+\mathbf{q}}(z)\times P(l,\mathbf{k};l',\mathbf{k}+\mathbf{q};\omega)\psi^*_{l',\mathbf{k}+\mathbf{q}}(z')\psi_{l,\mathbf{k}}(z'), \tag{9}$$

with

$$P(l,\mathbf{k};l',\mathbf{k}+\mathbf{q};\omega)\equiv\lim_{\gamma\to 0}\frac{n_F(E_{l,\mathbf{k}})-n_F(E_{l',\mathbf{k}+\mathbf{q}})}{E_{l,\mathbf{k}}-E_{l',\mathbf{k}+\mathbf{q}}+\hbar\omega+i\gamma}, \tag{10}$$

where n_F is the Fermi-Dirac function and the superscript * denotes the complex conjugation. The bare excitation satisfying the conservation of energy and momentum, i.e., the single-particle excitation (SPE) from the state $(l,\mathbf{k})$ to that $(l',\mathbf{k}+\mathbf{q})$, can occur as the denominator of the right-hand side (RHS) of Eq. (10) vanishes. It should be pointed out that the wave functions $\psi_{l,\mathbf{k}}(z)$ are included in the $\mathbf{k}$ and l summations of Eq. (9) to take into account the $\mathbf{k}$ dependence and the multisubband effect.

To determine the modes of the collective excitation, we take the Fourier expansion of $\epsilon_{\mathbf{q},\omega}(z;z')$ within a slab of thickness L which contains the well, and Eq. (8) reads

$$\epsilon^{\mathbf{q},\omega}_{m,n}=\delta_{m,n}-\sum_{m'} W^{q}_{m,m'}\Pi^{\mathbf{q},\omega}_{m',n}, \tag{11}$$

where the Fourier transforms are defined according to

$$\epsilon^{\mathbf{q},\omega}_{m,n}=\frac{1}{L}\int_{-L/2}^{L/2}dz\int_{-L/2}^{L/2}dz' e^{-ik_m z}\epsilon_{\mathbf{q},\omega}(z;z')e^{ik_n z'}, \tag{12}$$

with $k_n=2\pi n/L$. $W^{q}_{m,n}$ and $\Pi^{\mathbf{q},\omega}_{m,n}$ are the Fourier transforms calculated as in Eq. (12), but with $\epsilon_{\mathbf{q},\omega}(z,z')$ replaced by $W_q(z-z')$ and $\Pi_{\mathbf{q},\omega}(z;z')$, respectively. The modes of collective excitations, i.e., the eigenmodes of Eq. (11), are determined by the zeros of the determinant of this dielectric matrix, $\det[\epsilon^{\mathbf{q},\omega}_{m,n}]=0$.

III. RESULTS AND DISCUSSION

Based on the theoretical background described in the previous section, we calculated and will discuss in detail the magnetoplasmons of quantum wells under in-plane magnetic fields of various strengths, from extremely weak ($B\to 0$, $l_B \gg w$) to strong magnetic fields ($B=8$ T, $l_B \ll w$), at $T=0$ K. Two lowest spin-degenerate subbands are included in the calculation of the plasmon dispersion to take into account the possible coupling between the inter- and intrasubband excitations. To make the calculated results transparent, we first discuss those in two extreme situations, i.e., in weak and strong magnetic fields. The cases of intermediate **B** ($l_B \lesssim w$), which exhibit more complicated features, will be discussed later and analyzed in more details by a simplified two-layer model.

A. Plasmon dispersions

1. Weak magnetic fields

First, we calculate the plasmon dispersion and the SPE continuum of the quantum well for $B=0$ and show them in Fig. 3. The same result can be recovered also by the usual method of Refs. 13–15. Because of the large width of the well, the energy difference between the first ($c1$) and the second ($c2$) lowest subbands is small ($\Delta E_{12}\sim 1.1$ meV; see Fig. 1) and the frequencies of the intersubband ($c1$-$c2$) plasmons are low. Hence, the frequencies of the intrasubband plasmons can be comparable to those of the intersubband plasmons at finite q. A direct crossing of the two plasmon branches is observed at $q\sim 2.2\times 10^5$ cm^{-1} in Fig. 3. This is since the inversion symmetry of the quantum well structure makes the intra- and intersubband plasmons decoupled.[15] Since the subbands are parallel, the energies of the intersubband SPE's approach the value of ΔE_{12} and the width of the intersubband SPE's region shrinks to zero as $q\to 0$ (vertical excitations).

Next, we consider the quantum well subject to a weak in-plane magnetic field $B=0.2$ T. As shown in Fig. 1, the weak magnetic field slightly modifies the band dispersion for

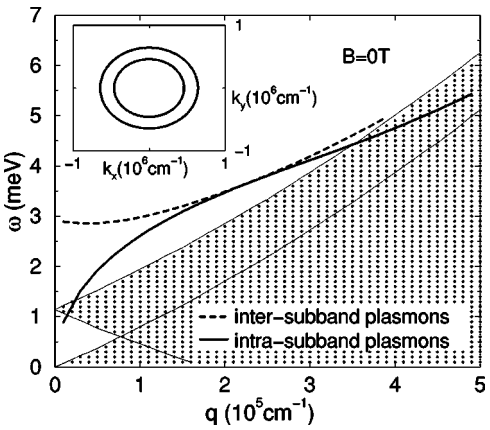

FIG. 3. Calculated plasmon dispersion of the quantum well for $B=0$ T. Dashed line: intersubband plasmons. Thick solid line: intrasubband plasmons. Upper hatched area: region of intersubband SPE's. Lower hatched area: region of intrasubband SPE's. Inset: corresponding Fermi contours.

$\mathbf{k}\|\mathbf{k}_x$; i.e., the dispersion of the subband $c1$ becomes flatter but the curvature of the subband $c2$ becomes larger. Consequently, the subbands of the quantum well under the in-plane B are nonparallel. The nonparallel subbands allow more intersubband SPE's with various excitation energies even for $q\to 0$. Therefore, unlike the case without magnetic field, one can notice a finite width of the intersubband SPE's for $q=0$ in Fig. 4(a).

We also see in Fig. 4(a) a pronounced anticrossing feature in the plasmon dispersions for $B=0.2$ T and $\mathbf{q}\|\mathbf{k}_x$. This indicates that the in-plane magnetic field induces a coupling between the intra- and intersubband plasmons in the *symmetric* quantum well. It is well known that such a coupling of plasmons in quantum wells without **B** can be induced only as the inversion symmetry of wells is broken.[15] In the presence of **B**, the wave functions for $k_x\neq 0$ cannot remain symmetric because the middle point of V_B is shifted to $z_0=-k_x l_B^2\neq 0$ (the middle points of V_{QW} and V_H stay at $z=0$) and the total confinement potential $V_{conf}=V_{QW}+V_H+V_B$ is asymmetric for $k_x\neq 0$. Due to the corresponding asymmetry of wave functions, the coupling between the inter- and intrasubband plasmons in Fig. 4 results.

As the magnetic field is raised to higher values, the subbands become more nonparallel and the region of the intersubband SPE broadens more. The plasmon dispersion of the quantum well for $B=1$ T is shown in Fig. 4(b). The region of SPE's is so wide that all intersubband plasmons are Landau damped in the SPE region and vanish. As a result, only one branch of the intrasubband plasmons is left in the narrow energy gap between the continuum of the intra- and intersubband SPE's, with energies less than 1.3 meV. To make more modes of intrasubband plasmons emerge, one can further increase the magnitude of B to raise the energy of the second subband and to enlarge the energy gap between the intra- and intersubband SPE's.

2. Strong magnetic fields

As a typical example for strong fields, we consider the case of $B=8$ T ($l_B\approx 9$ nm), in which two Fermi contours

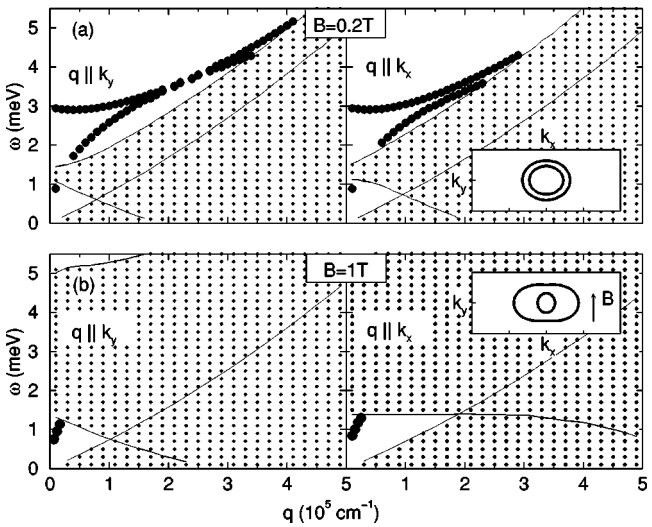

FIG. 4. Calculated plasmon dispersion of the quantum well subject to (a) $B=0.2$ T and (b) $B=1$ T in the y direction for the in-plane plasmon wave vector $\mathbf{q}\|\mathbf{B}$ (left) and $\mathbf{q}\perp\mathbf{B}$ (right). Solid circles: plasmon dispersions. Upper (lower) hatched area: region of intersubband (intrasubband) SPE's.

are formed with finite separation $2|k_x|\sim 3.6\times 10^6$ cm^{-1} (see the inset of Fig. 5). Hence, no electrons occupy the central part of the well where $|z_0|=l_B^2|k_x|<14.5$ nm and only states with $|z_0|>14.5$ nm are occupied on both sides of the well. The narrow spatial layers occupied by electrons with small l_B lead to a minor overlap between the wave functions localized on different sides of the well. In this situation the single quantum well behaves completely like a *two-component* system. Figure 6 shows the total density distribution of the electrons in the quantum well in various B to manifest such a one- to two-component transition.

The one- to two-component transition significantly affects the features of the collective excitations. As shown in Fig. 5, the plasmon dispersion of the *single* well in the strong magnetic field has the typical features of a two-component system, like a double quantum well,[23] with the emergence of the undamped AP's with a quasilinear dispersion, beside the usual intrasubband OP's, for any in-plane direction of **q**.[23–30] In the two-component limit, the thorough depression of the overlap between the electron layers on the both sides of the well makes out-of-phase motions (the acoustic modes) of the charge density waves in both layers possible.

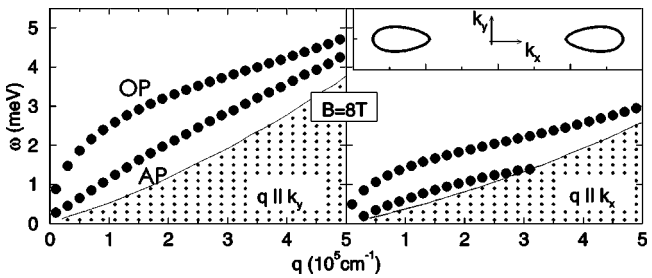

FIG. 5. Calculated plasmon dispersion of the quantum well subject to $B=8$ T in the y direction for the in-plane plasmon wave vector $\mathbf{q}\|\mathbf{B}$ (left) and $\mathbf{q}\perp\mathbf{B}$ (right).

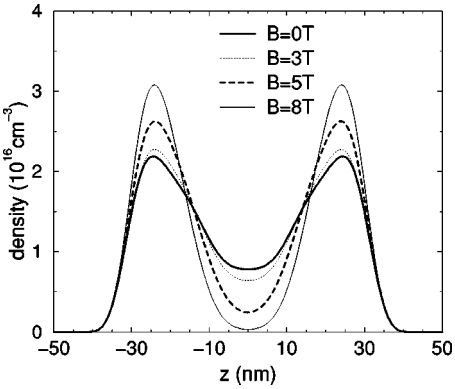

FIG. 6. Total density distributions of the electrons in the quantum well subject to in-plane magnetic fields with various magnitudes.

3. Intermediate magnetic fields

Between the above two limits, intermediate **B** can induce an interesting anisotropy effect. The calculated plasmon dispersions for $B=2$ and 3 T are shown in Fig. 7. We find that two branches of the intrasubband plasmons exist for $\mathbf{q}\|\mathbf{k}_y$, whereas only one remains for $\mathbf{q}\|\mathbf{k}_x$. Figure 8 shows the plasmon modes in these cases for various angles θ between **q** (with constant $|\mathbf{q}|$) and **B**, in the range from 0 to 0.5π (the θ values, not covered by the above range, can be straightforwardly transformed into this range according to the symmetry of Fermi contours). For $B=2$ T (3 T) and $|\mathbf{q}|=5\times 10^4$ cm^{-1} ($|\mathbf{q}|=10^5$ cm^{-1}), only one branch of the intrasubband plasmons exists for large angles between **q** and **B**, i.e., $0.25\pi<\theta<0.5\pi$ ($0.45\pi<\theta<0.5\pi$), whereas two branches of the undamped optical and acoustic plasmons can be observed for small angles between **q** and **B**, $0<\theta<0.25\pi$ ($0<\theta<0.45\pi$). This suggests that, just by tuning the direction of applied in-plane **B** field, manipulating the number of the plasmon branches for some given **q** becomes possible in experiments.

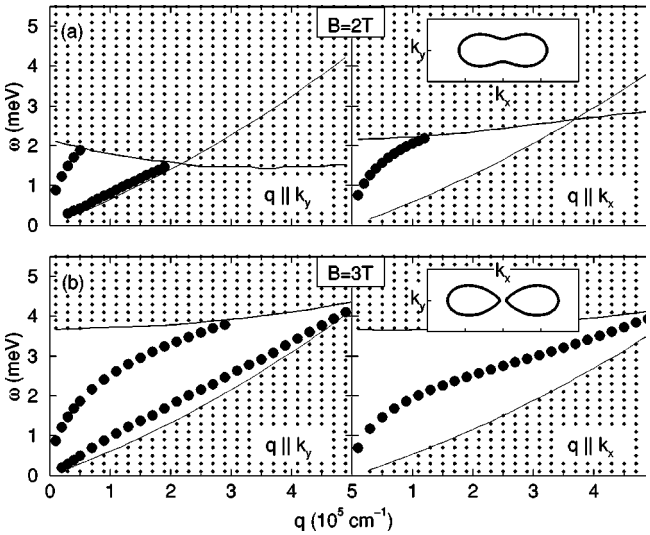

FIG. 7. Calculated plasmon dispersion of the quantum well subject to (a) $B=2$ T and (b) $B=3$ T in the y direction, for the in-plane plasmon wave vectors $\mathbf{q}\|\mathbf{B}$ (left) and $\mathbf{q}\perp\mathbf{B}$ (right).

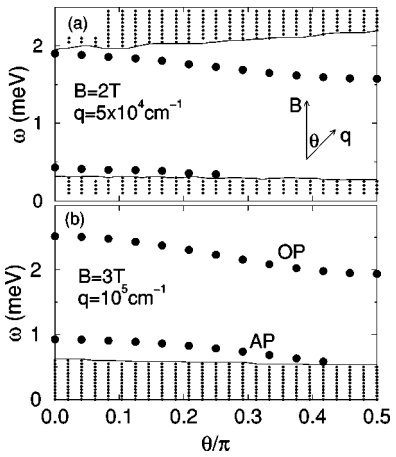

FIG. 8. Dispersion of plasmon modes for **q** with fixed magnitude q along various in-plane directions in the presence of **B**. θ is the angle between **B** and **q**.

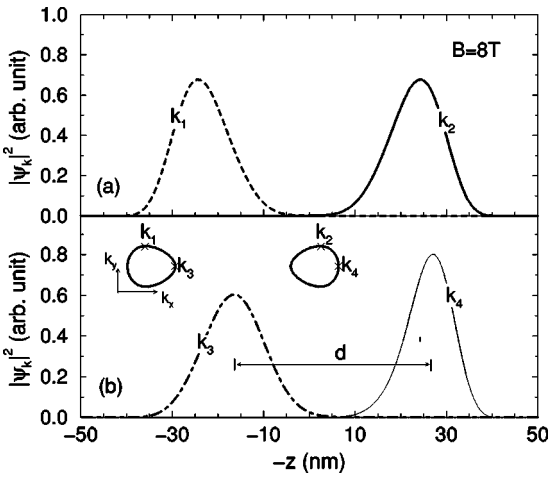

FIG. 9. The square of the wave functions of the dominant states of the quantum well subject to $B=8$ T. Inset: sketch of the corresponding Fermi contours and the positions of the dominant states.

4. Analysis

A full analytic analysis for the above unusual anisotropic feature of the magnetoplasmons is difficult because of the complicated electronic structure. However, the results become plausible, if some simplifying assumptions are made concerning the states which dominate the dielectric response of the quantum well with in-plane field **B**. First, we assume that, for in-plane magnetic fields with sufficiently strong magnitude, the electrons localized on the both sides of the well can be modeled by two electrostatically coupled, but electronically separated layers. Second, we assume that the dielectric response of each layer is dominated by the states near (in **k** space) the characteristic state (on the Fermi contour) which, for the considered **q** vector, yields the *largest* contribution to the polarization [Eq. (9)]. For intrasubband excitations, this dominant contribution comes from the allowed intrasubband SPE $(c1,\mathbf{k})\rightarrow(c1,\mathbf{k}+\mathbf{q})$ with $n_F(E_{c1},\mathbf{k})-n_F(E_{c1},\mathbf{k}+\mathbf{q})\neq 0$, which makes the denominator $\hbar\omega-(E_{c1,\mathbf{k}+\mathbf{q}}-E_{c1,\mathbf{k}})$ of Eq. (9) smallest [it must be positive for undamped excitations $(\mathbf{q},\ \omega)$]. In the long-wavelength limit, the characteristic state is that state on the Fermi contour that yields *maximum* SPE energy, $E_{c1,\mathbf{k}+\mathbf{q}}-E_{c1,\mathbf{k}}$ (for parabolic band structure $E_{c1,\mathbf{k}}=\hbar^2k^2/2m^*+E_{c1,\mathbf{0}}$, this is the state with $\mathbf{k}=k_F\mathbf{q}/|\mathbf{q}|$). Third, we assume that the Fermi velocities at the characteristic states of both layers determine the number of undamped collective excitations of the double-layer system for given **q**, just as they do for purely electrostatically coupled double-quantum-well systems with parabolic and isotropic band structures in each well.[23]

This simplified model allows a further analysis, based on the available theory for usual two-component systems, like 2D electron double layers without magnetic fields. It has been shown that undamped acoustic plasmons of double layers can emerge only if the layer separation d is above a critical distance d_c, which strongly depends on the Fermi velocities of layers.[23,25] According to the work of Santoro and Giuliani,[23] which, within the RPA, takes into account the exact expression for the polarization function and the group velocities of acoustic modes for double-layer systems with isotropic and parabolic band structure, the critical distance is given by

$$d_c=d_0\frac{(1-s^2)^{1/2}}{1-(1-s^2)^{1/2}}, \tag{13}$$

with $d_0\equiv\kappa a_B m_0/4m_2^*$ and $s\equiv v_{F2}/v_{F1}$ $(v_{F1}>v_{F2})$, where v_{Fi} (m_i^*) is the Fermi velocity (effective mass) for layer i, and a_B denotes the effective Bohr radius. Equation (13) indicates that, if the Fermi velocities of the two ideal 2D layers are identical, the undamped acoustic plasmons can always exist due to the vanishing of d_c. In contrast, a finite value of d_c is caused by a difference between the Fermi velocities of the two layers and increases as the ratio $v_{F2}/v_{F1}(\leqslant 1)$ decreases.

First, we apply the model to the case of strong field $B=8$ T. We numerically determine the characteristic states that are involved in the allowed SPE with maximum energy. The two separated Fermi contours yield two characteristic states, respectively belonging to both Fermi contours, for some considered **q**. The positions of these states in the **k** space are schematically shown in the lower inset of Fig. 9 and the in-plane wave vectors of the characteristic states for $\mathbf{q}\|\mathbf{k}_y$ $[\mathbf{q}\|\mathbf{k}_x]$ are denoted as $\mathbf{k}_1$ and $\mathbf{k}_2$ ($\mathbf{k}_3$ and $\mathbf{k}_4$), respectively. One can notice that these are the states on the respective Fermi contours with the largest k_y (k_x) components for $\mathbf{q}\|\mathbf{k}_y$ $[\mathbf{q}\|\mathbf{k}_x]$, i.e., the states on the Fermi contours with $\mathbf{k}\|\mathbf{q}$. The square of the wave functions of these characteristic states is shown in Fig. 9. We see that the wave functions are strongly localized on both sides of the well (because of the small l_B value) and the overlap between those of the states with wave vectors $\mathbf{k}_1$ and $\mathbf{k}_2$ ($\mathbf{k}_3$ and $\mathbf{k}_4$) is very small, like those of the usual double-layer systems (without **B**). In this situation, our simplified model is very suitable to describe a quantum well subject to a strong **B**.

To evaluate the d_c within our model, we numerically calculate the Fermi velocities of these relevant states and obtain the ratio of the Fermi velocities, $v_{\mathbf{k}_1}/v_{\mathbf{k}_2}=1$ and $v_{\mathbf{k}_3}/v_{\mathbf{k}_4}$

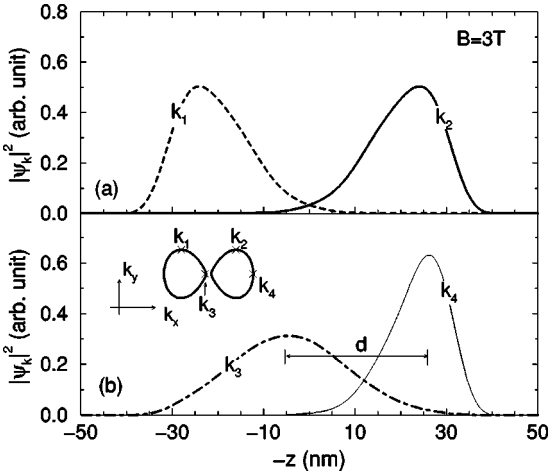

FIG. 10. The square of the wave functions of the dominant states of the quantum well subject to $B=3$ T. Inset: sketch of the corresponding Fermi contours and the positions of the dominant states.

≈ 0.38. The corresponding critical distance d_c, calculated according to Eq. (13) with $m_i^*=0.067m_0$, is $d_c=0$ [$d_c \approx 30$ nm], for $\mathbf{q}\|\mathbf{k}_y$ [$\mathbf{q}\|\mathbf{k}_x$]. The zero d_c accounts for the emergence of the undamped acoustic plasmons for $\mathbf{q}\|\mathbf{k}_y$ in Fig. 5. For $\mathbf{q}\|\mathbf{k}_x$, the d_c value is finite but still less than the average distance between the dominant states $\mathbf{k}_3$ and $\mathbf{k}_4$, $d \approx 45$ nm (see Fig. 9), and two branches of undamped plasmons can exist for $\mathbf{q}\|\mathbf{k}_x$, as shown in Fig. 5.

In the same way, we can analyze the case of $B=3$ T to understand the origin of the anisotropy of branch number of plasmons. We numerically determine the characteristic states for $B=3$ T and show their positions (in the $\mathbf{k}$ space) in the lower inset of Fig. 10. The in-plane wave vectors of these states for $\mathbf{q}\|\mathbf{k}_y$ [$\mathbf{q}\|\mathbf{k}_x$] are denoted as $\mathbf{k}_1$ and $\mathbf{k}_2$ [$\mathbf{k}_3$ and $\mathbf{k}_4$], as in the case of $B=8$ T. Basically, the Fermi contours for B above 3 T have similar features, which are two separated contours, symmetrically placed on both sides of the k_y axis. The determined characteristic states for $B=3$ T are therefore also those states on the corresponding Fermi contour, possessing the maximum value of the k_y (k_x) for $\mathbf{q}\|\mathbf{k}_y$ [$\mathbf{q}\|\mathbf{k}_x$]. But a remarkable difference from the case of a stronger **B** field is that the state with $\mathbf{k}=\mathbf{k}_3$ is very near to the saddle point of the $\mathbf{k}$ origin and has particularly low Fermi velocity. The low Fermi velocity of this state leads to a low value $v_{\mathbf{k}_3}/v_{\mathbf{k}_4} \approx 0.25$ and large d_c (≈ 76 nm) for $\mathbf{q}\|\mathbf{k}_x$, whereas the value of $v_{\mathbf{k}_1}/v_{\mathbf{k}_2}$ remains unity and $d_c=0$ for $\mathbf{q}\|\mathbf{k}_y$. Because of zero d_c, there still exist two branches of the undamped plasmons for $\mathbf{q}\|\mathbf{k}_y$ in Fig. 7(b). The large value of d_c (≈ 76 nm) for $\mathbf{q}\|\mathbf{k}_x$ is much larger than the average distance between the wave functions of $\mathbf{k}_3$ and $\mathbf{k}_4$, $d \approx 30$ nm (see Fig. 10), and prohibits the existence of the acoustic mode, and only one mode is left [see Fig. 7(b)].

Comparing Fig. 9 with Fig. 10, one can notice that the wave functions become broader with decreasing B, so that the corresponding densities overlap in Fig. 10. One should note, however, that we consider here exact wave functions $\Psi_{c1,\mathbf{k}}(\mathbf{r},z)$ of the full Hamiltonian H, Eq. (1), which are orthogonal, $\langle \Psi_{c1,\mathbf{k}} | \Psi_{c1,\mathbf{k}'} \rangle = \delta_{\mathbf{k},\mathbf{k}'}$, and have vanishing matrix elements $\langle \Psi_{c1,\mathbf{k}} | H | \Psi_{c1,\mathbf{k}'} \rangle = 0$ for $\mathbf{k} \neq \mathbf{k}'$. This situation is very different from that of bilayers without **B**, often considered in the literature,[27] where one starts with eigenfunctions of the isolated individual layers and considers the tunneling effect by introducing the parameter $\Delta_{SAS}(=E_{c2}-E_{c1})$, the tunneling-induced energy gap between symmetric $(c1)$ and antisymmetric $(c2)$ states. The energy gap Δ_{SAS} eventually leads to a rise of the acoustic plasmon dispersion to finite energies (higher than Δ_{SAS}) in the long-wavelength limit.[27,28] In contrast to those phenomenological approaches, in our treatment all possible tunneling effects are already included in the self-consistent band structure calculation.

With weaker **B**, the behavior of the dielectric response of the quantum well approaches the one-component limit and our simplified model no longer describes the system very well. In the case of $B=2$ T, a peanutlike Fermi contour is formed, instead of two separated ones [see the inset of Fig. 7(a)]. This means that some electrons, with $z_0 \sim 0$, occupy the central part of the well. Hence, the system in this situation does not behave completely like a two-component system. For $\mathbf{q}\|\mathbf{k}_y$, we still find two states that can generate the largest polarization and the maximum energy of SPE. These are the states with the maximum value of the k_y among the states on the Fermi contour and possess the same Fermi velocity, similar to the states of $\mathbf{k}_1$ and $\mathbf{k}_2$ mentioned previously. The overlap of the corresponding wave functions is still relatively small, and the existence of two plasmons in this situation seems reasonable within our simplified model. However, the situation for $\mathbf{q}\|\mathbf{k}_x$ is different. On the single Fermi contour, many SPE's are allowed in the half-plane of $k_x>0$ and yield larger polarizations, while only a few SPE's are allowed for $k_x<0$ and their contribution to the polarization is not comparable to those for $k_x>0$. As a result, only one characteristic state that yields the SPE with the maximum energy for $\mathbf{q}\|\mathbf{k}_x$ can be determined. Its wave vector possesses the maximum k_x component among the states on the Fermi contour, similar to the state of $\mathbf{k}_4$ in the previous cases with higher **B** (however, the state of $\mathbf{k}_3$ in the previous cases does not exist in this case because of the single Fermi contour, instead of two). Hence, the dielectric response of the quantum well with $B=2$ T for $\mathbf{q}\|\mathbf{k}_x$ is dominated only by the sole characteristic state and the plasmon dispersion exhibits a typical feature of one-component systems, i.e., only one branch of undamped intrasubband plasmons. With still lower magnetic fields, the quantum well completely becomes a one-component system (one branch of intrasubband plasmons exists for $\mathbf{q}$ in any in-plane direction) and our simplified model is not suitable for the analysis.

B. Charge density waves

In this section, the symmetry of charge density of the collective excitations will be discussed. First, we consider the collective excitations with $\mathbf{q}=(0,q,0)\|\mathbf{B}$. In this case, we can replace $\psi_{\mathbf{k}+\mathbf{q}}(z)$ in the $\mathbf{k}$ summation of Eq. (9) with $\psi_{k_x}(z)$, because $\psi_{\mathbf{k}+\mathbf{q}}(z)=\psi_{k_x+q_x}(z)$ is independent of the k_y component of the wave vector and the q_x component of the $\mathbf{q}$ is zero. Exploiting the relations that $V_B(k_x;z)=V_B$

$(-k_x;-z)$ [see Eq. (3)], $V_H(z)=V_H(-z)$ and $V_{QW}(z)=V_{QW}(-z)$ in Eq. (2) for the symmetric well under $\mathbf{B}=(0,B,0)$, we have $\psi_{k_x}(z)=\psi_{-k_x}(-z)$. Then, taking the transformation $k_x\rightarrow -k_x$ again in the $\mathbf{k}$ summation of Eq. (9) and exploiting that $\psi_{k_x}(z)=\psi_{-k_x}(-z)$, we can derive $\Pi(z,z')=\Pi(-z,-z')$. According to Eq. (8), we can straightforwardly derive

$$\epsilon(z,z')=\epsilon(-z,-z') \tag{14}$$

for $\mathbf{q}\|\mathbf{B}$. Equation (14) indicates that the matrix elements of $\epsilon(z,z')$ in the Fourier basis fulfill $\epsilon_{m,n}=\epsilon_{-m,-n}$ [see Eq. (12)]. Therefore, the components of the corresponding eigenstates $\mathbf{V}^{sc}$ $(\Sigma_n \epsilon_{m,n}V_n^{sc}=0)$ satisfy $V_n^{sc}=\pm V_{-n}^{sc}$. The latter equation means that $V^{sc}(z)$ is either a *symmetric* or an *antisymmetric* function of z. Because the polarization function fulfills $\Pi(z,z')=\Pi(-z,-z')$, the distribution of the charge density waves of the collective excitations $[n^{ind}(z)=\int dz'\Pi(z,z')V^{sc}(z')]$ (Ref. 19) is either *symmetric* or *antisymmetric*,[12] which, respectively, correspond to the in-phase and out-of-phase oscillations of plasmon modes, i.e., optical and acoustic modes, for low-frequency excitations in a two-component system.[23] In contrast, for $\mathbf{q}=(q,0,0)\perp\mathbf{B}$, $\psi_{\mathbf{k}+\mathbf{q}}(z)=\psi_{k_x+q}(z)\neq\psi_{k_x}(z)$ because $q_x\neq 0$. This leads to $\epsilon(z,z')\neq\epsilon(-z,-z')$. It indicates that the symmetry of charge density waves of the collective excitations with wave vector $\mathbf{q}$ is destroyed by the $\mathbf{B}$ $(\perp\mathbf{q})$.[12]

The above relation between the (anti)symmetry of collective charge density and the direction of $\mathbf{q}$ with respect to $\mathbf{B}$ has also been deduced from the analysis of the work of Ref. 12 for the case of the symmetric double quantum well. According to our analysis, one further recognizes that the relation directly results from the symmetry of 2DES and is valid also for other symmetric structures. We shall show in the next section that such a (anti)symmetry or a broken symmetry of the charge density for different $\mathbf{q}$ can yield different features of the optical response to external polarized fields.

C. Absorption spectra

For the 2D system subjected to an external longitudinal electric field with in-plane wave vector $\mathbf{q}$ and frequency ω, the average power dissipation per unit area in the screened system is expressed as (see Ref. 19 for details)

$$\overline{P}=-\frac{\omega}{2}\mathrm{Im}\int dz[V^{ex}_{\mathbf{q},\omega}(z)]^* n^{ind}_{\mathbf{q},\omega}(z) \tag{15}$$

[another equivalent expression, appearing in Ref. 19, is that of Eq. (15) with the replacement $V^{ex}_{\mathbf{q},\omega}$ by $V^{sc}_{\mathbf{q},\omega}$].[31] Following the derivation of Ref. 19, we have the normalized power dissipation with respect to the Fourier component of external potential $V_n^{ex}e^{iq_z z}$ with $q_z=2\pi n/L$,

$$\overline{p_n}\propto\omega\,\mathrm{Im}\sum_m [W_q^{-1}]_{n,m}(\epsilon^{-1}_{\mathbf{q},\omega})_{m,n}, \tag{16}$$

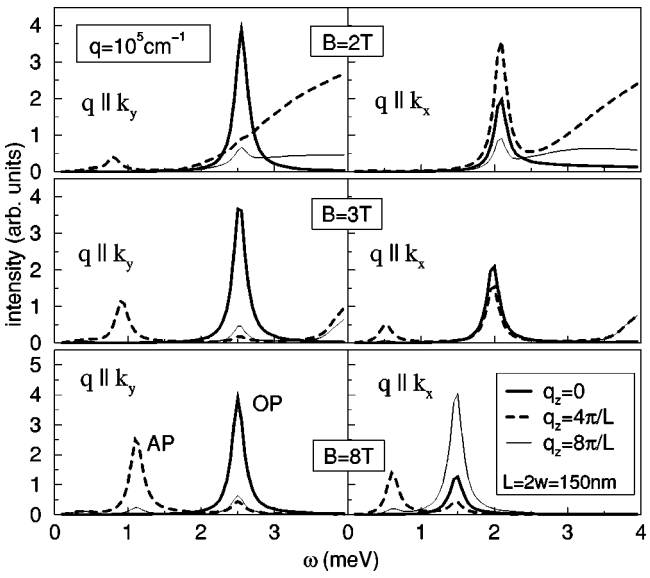

FIG. 11. Calculated energy-loss spectra of the quantum well, for $q=10^5$ cm^{-1} with the orientation of the $\mathbf{k}_x$ and $\mathbf{k}_y$ directions, under the in-plane magnetic fields in the y direction with magnitude $B=2$ T, 3 T, and 8 T.

where $[W_q^{-1}]_{n,m}$ is the element of the inverse matrix of $W^q_{m,n}$ and $(\epsilon^{-1}_{\mathbf{q},\omega})_{m,n}$ is that of the inverse matrix of $\epsilon^{\mathbf{q},\omega}_{m,n}$. In the calculation of absorption spectra, a typical value of the phenomenological parameter $\gamma=0.1$ meV is taken in Eq. (9) to model the damping mechanism.[15,32] Figure 11 shows the calculated energy-loss spectra of the quantum well for various magnitudes of $\mathbf{B}$ in the y direction, including $B=2$ T, 3 T, and 8 T, for $\mathbf{q}$ $(|\mathbf{q}|=10^5$ cm$^{-1})$ in the $\mathbf{k}_x$ and the $\mathbf{k}_y$ directions and various q_z.

For $B=2$ T and $\mathbf{q}\|\mathbf{k}_x$, only a sharp peak corresponding to the optical plasmon at $\omega\approx 2.1$ meV appears in the spectrum. For $\mathbf{q}\|\mathbf{k}_y$, in addition to the signal of the Landau-damped optical plasmon at $\omega\approx 2.1$ meV, a weak absorption peak at $\omega\approx 0.8$ meV induced by the undamped acoustic plasmon is observed. The appearance of the strong absorption corresponding to the optical plasmon for $\mathbf{q}\|\mathbf{k}_y$ and $q_z=0$, which according to Fig. 7(a) is expected to be Landau damped, indicates that the collective excitation of the optical mode seems to be decoupled from the intersubband SPE. In fact, a constant external field (a field containing only the component for $q_z=0$) cannot induce an intersubband SPE for $\mathbf{q}=(0,q,0)\|\mathbf{k}_y$, because the matrix element vanishes due to orthogonality of the k_x-dependent wave functions $(\langle c1,\mathbf{k}|V^{ex}|c2,\mathbf{k}+\mathbf{q}\rangle=V^{ex}\langle c1,k_x|c2,k_x+q_x\rangle\propto\langle c1,k_x|c2,k_x\rangle=0)$. Hence, there occurs no absorption due to SPE's in the range of the energies of intersubband SPE's for $\mathbf{q}\|\mathbf{k}_y$ and $q_z=0$, and the peak due to the excitation of the collective optical mode is undamped. The same phenomenon can also be found in the case of other $\mathbf{B}$ fields (see that of $B=3$ and 8 T for q in the $\mathbf{k}_y$ direction in Fig. 11). For $\mathbf{q}\|\mathbf{k}_y$ and $q_z\neq 0$ $[V^{ex}\propto\exp(iq_z z)]$, the orthogonality of wave functions does not lead to the vanishing of the matrix element $\langle c1,k_x|V^{ex}|c2,k_x\rangle$ and a finite absorption due to SPE's results in the range of energies of intersubband SPE's $(\omega\gtrsim 2$ meV).

For $B=3$ T, there exist two absorption peaks corresponding to the undamped (damped) acoustic and optical plasmons for $\mathbf{q}$ in the $\mathbf{k}_y$ [$\mathbf{k}_x$] direction. In the strong magnetic field $B=8$ T, as a case of the two-component limit, two pronounced signals of the undamped acoustic and optical plasmons appear in the spectra for any direction of $\mathbf{q}$. In addition to the previous magnetotransport measurement,[17] we predict here that an optical measurement can also offer evidence for the existence of the one- to two-component transition induced by in-plane magnetic fields.

It is also found that the intensity of absorption strongly depends on the Fourier component of the applied electric field. For $\mathbf{q}\|\mathbf{B}$ in the $\mathbf{k}_y$ direction, the absorption signal of the acoustic plasmons for the $q_z=0$ component vanishes and the strongest absorption signal results as the wavelength of the external field, $\lambda_z=2\pi/q_z$, is equal to the well width ($w=75$ nm), i.e., $\lambda_z=w$. Thus, in the cases of Fig. 11 for $\mathbf{q}$ in the $\mathbf{k}_y$ direction, the absorption signals for the acoustic plasmons have the strongest intensity for $q_z=4\pi/L$ ($L=150$ nm, i.e., $\lambda_z=75$ nm) and decay as q_z becomes smaller or larger. In contrast, the strongest signal of the optical plasmon is that for the $q_z=0$ component and a minimum absorption signal occurs as $q_z=4\pi/L$ (the large absorption intensity of the optical plasmon for $\mathbf{q}\|\mathbf{k}_y$ and $q_z=4\pi/L$ in the case of $B=2$ T is mainly induced by the intersubband SPE's). For brevity, we only show the spectra for these critical $q_z(=0,4\pi/L)$ and that for $q_z=8\pi/L$ for comparison in Fig. 11. The feature of the spectrum for other q_z can be qualitatively understood by means of interpolation. Such q_z dependences of the absorption intensities exist, however, only for $\mathbf{q}\|\mathbf{k}_y$. For $\mathbf{q}\|\mathbf{k}_x$, one cannot find a regular relation between the absorption intensities and q_z.

Due to a lack of analytical formulation describing the collective excitations and the induced charge density, an analysis for the numerically calculated absorption spectra, including the q_z dependence of absorption intensity, is difficult. However, exploiting the fact that the induced charge density possesses some certain symmetry (with respect to z) as $\mathbf{q}\|\mathbf{k}_y$ (see the previous section), a further analysis for the case of $q_z=0$ becomes possible. Exploiting Eq. (15), one can explain the vanishing of the absorption of acoustic modes for $\mathbf{q}\|\mathbf{k}_y$ and $q_z=0$, as shown in Fig. 11. Because an external potential, containing only the component of $q_z=0$, is an even function of z (a constant) and the induced charge density, $n^{ind}_{\mathbf{q},\omega}(z)$, of an acoustic mode for $\mathbf{q}\|\mathbf{k}_y$ is an odd (antisymmetric) function with respect to z, Eq. (15) vanishes after the integration and no absorption occurs in that case. In contrast, the strength of absorption signals of optical modes for $\mathbf{q}\|\mathbf{k}_y$ and any q_z is finite, because the Fourier component of the external potential, $V_n^{ex}\exp(ik_nz)$, with respect to $q_z=k_n$ always contains an even function $V_n^{ex}\cos(k_nz)$ and the induced charge density is also an even (symmetric) function with respect to z. For $\mathbf{q}\|\mathbf{k}_x$, it is, however, hard to perform the same analysis because the symmetry or the antisymmetry of the charge density of the collective excitations does not exist.

IV. CONCLUSIONS

In conclusion, we have presented a complete investigation of the collective excitations in symmetric wide quantum wells subject to in-plane magnetic fields, which treats the magnetic-field-induced nonparabolicity and the wave-vector dependence of the subband wave functions in the framework of the RPA exactly. The calculated results, including the plasmon dispersion, the single-particle excitations, and energy-loss spectra, show that in-plane magnetic fields significantly affect the basic feature of the collective excitations. One of the remarkable magnetic-field-induced effects is the one- to two-component transition in the collective excitations. In strong magnetic fields, the plasmon dispersion has, surprisingly, the typical features of a two-component system with the existence of an optical as well as an acoustic plasmon branch for any in-plane direction of $\mathbf{q}$, whereas there exists only one branch of intrasubband plasmons for very low magnetic fields B. In intermediately high magnetic fields, the number of the plasmon branches for some given in-plane wave vector depends on the direction of the in-plane magnetic field. For $\mathbf{q}\perp\mathbf{B}$, one branch of the intrasubband plasmons exists like in the cases of weak magnetic fields. In contrast, for $\mathbf{q}\|\mathbf{B}$, the plasmons behave like in a two-component system and two branches of the intrasubband plasmons (OP's and AP's) emerge. Hence, through changing the direction of applied intermediate magnetic fields, varying the number of the plasmon branches of wide quantum wells for some given $\mathbf{q}$ becomes possible. These calculated results of the magnetoplasmons are further analyzed by a simplified double-layer model based on the theory of Ref. 23, providing a transparent analytical formulation to determine the emergence of the acoustic mode in a two-component system. The analysis successfully clarifies the emergence of the acoustic modes due to the in-plane $\mathbf{B}$ field above the intermediate regime. For a weak magnetic field ($B=2$ T) and a longitudinal electric field with the wave vector $\mathbf{q}\|\mathbf{B}$ and $q_z=0$, we find sharp absorption lines due to optical plasmons in the energy range of intersubband SPE's. We explain this phenomenon in terms of a decoupling of collective and single-particle excitations due to symmetry properties.

In this work we have not considered exchange and correlation effects and, as a consequence, we have not discussed spin-density excitations. In view of the controversial literature about collective spin states in double-layer systems,[28,33,34] it might be interesting to generalize our work to include spin effects. In principle it should be possible to generalize our work within the Hartree and RPA to calculations within the local density approximation (LDA) and time-dependent LDA, respectively, or to the corresponding spin-density versions.

ACKNOWLEDGMENT

S.J.C. acknowledges support from the Deutscher Akademischer Austauschdiest (DAAD).

[1] J. Smoliner, W. Demmerle, G. Berthold, E. Gornik, G. Weimann, and W. Schlapp, Phys. Rev. Lett. **63**, 2116 (1989).
[2] K.-M. Hung and G. Y. Wu, Phys. Rev. B **45**, 3461 (1992).
[3] T. Jungwirth, T. S. Lay, L. Smrcka, and M. Shayegan, Phys. Rev. B **56**, 1029 (1997).
[4] G. Salis, B. Ruhstaller, K. Ensslin, K. Campman, K. Maranowski, and A. C. Gossard, Phys. Rev. B **58**, 1436 (1998).
[5] S. K. Lyo, N. E. Harff, and J. A. Simmons, Phys. Rev. B **58**, 1572 (1998).
[6] D. Huang and S. K. Lyo, Phys. Rev. B **59**, 7600 (1999).
[7] A. Hernández-Cabrera, P. Aceituno, and F. T. Vasko, Phys. Rev. B **60**, 5698 (1999).
[8] L. V. Kulik, I. V. Kukushkin, V. E. Kirpichev, K. v. Klitzing, and K. Eberl, Phys. Rev. B **61**, 1712 (2000).
[9] A. Wixforth, M. Kaloudis, C. Rocke, K. Ensslin, M. Sundaram, J. H. English, and A. C. Gossard, Semicond. Sci. Technol. **9**, 215 (1994).
[10] J. Dempsey and B. I. Halperin, Phys. Rev. B **45**, 3902 (1992).
[11] P. I. Tamborenea and S. Das Sarma, Phys. Rev. B **49**, 16 593 (1994).
[12] G. R. Aizin and G. Gumbs, Phys. Rev. B **54**, 2049 (1996).
[13] B. Vinter, Phys. Rev. B **15**, 3947 (1977).
[14] S. Das Sarma, Phys. Rev. B **29**, 2334 (1984).
[15] J. K. Jain and S. Das Sarma, Phys. Rev. B **36**, 5949 (1987).
[16] R. H. J. De Meester and F. M. Peeters, J. Phys.: Condens. Matter **11**, 6207 (1999).
[17] T. S. Lay, T. Jungwirth, L. Smrcka, and M. Shayegan, Phys. Rev. B **56**, R7092 (1997).
[18] S. J. Cheng and R. R. Gerhardts, Solid State Commun. **116**, 669 (2000).
[19] S. J. Cheng and R. R. Gerhardts, Phys. Rev. B **63**, 035314 (2001).
[20] H. Ehrenreich and M. H. Cohen, Phys. Rev. **115**, 786 (1959).
[21] S. K. Lyo, Phys. Rev. B **50**, 4965 (1994).
[22] P. M. Koenraad, A. B. Henriques, A. F. W. van de Stadt, and J. H. Wolter, Physica B **256-258**, 229 (1998).
[23] G. E. Santoro and G. F. Giuliani, Phys. Rev. B **37**, 937 (1988).
[24] G. Fasol, N. Mestres, H. P. Hughes, A. Fischer, and K. Ploog, Phys. Rev. Lett. **56**, 2517 (1986).
[25] S. Das Sarma and A. Madhukar, Phys. Rev. B **23**, 805 (1981).
[26] P. I. Tamborenea and S. Das Sarma, Phys. Rev. B **49**, 16 821 (1994).
[27] S. Das Sarma and E. H. Hwang, Phys. Rev. Lett. **81**, 4216 (1998).
[28] P. G. Bolcatto and C. R. Proetto, Phys. Rev. Lett. **85**, 1734 (2000).
[29] D. S. Kainth, D. Richards, H. P. Hughes, M. Y. Simmons, and D. A. Ritchie, Phys. Rev. B **57**, R2065 (1998).
[30] D. S. Kainth, D. Richards, A. S. Bhatti, H. P. Hughes, M. Y. Simmons, E. H. Linfield, and D. A. Ritchie, Phys. Rev. B **59**, 2095 (1999).
[31] Replacing $V^{ex}(z)$ with $[V^{sc}(z)-V^{ind}(z)]$ in Eq. (15), the term involving $V^{ind}(z)$ is real and can be omitted in the equation, because $\int dz[V^{ind}_{\mathbf{q},\omega}(z)]^* n^{ind}_{\mathbf{q},\omega}(z)$ is equivalent to $\int dz \int dz' [n^{ind}_{\mathbf{q},\omega}(z')]^* V_q(z-z') n^{ind}_{\mathbf{q},\omega}(z)$ according to Eq. (5) and the latter is invariant after taking the operation of complex conjugation. Therefore, Eq. (15) can also be expressed as $\overline{P} = (-\omega/2)\,\mathrm{Im} \int dz [V^{sc}_{\mathbf{q},\omega}(z)]^* n^{ind}_{\mathbf{q},\omega}(z)$.
[32] J. K. Jain and P. B. Allen, Phys. Rev. B **32**, 997 (1985).
[33] F. A. Reboredo and C. R. Proetto, Phys. Rev. Lett. **79**, 463 (1997).
[34] Z. Wilamowski and W. Jantsch, in *Proceedings of the 25th International Conference on the Physics of Semiconductors, Osaka, 2000*, edited by N. Miura and T. Ando (Springer-Verlag, Berlin, 2001), p. 985.